

Calculating charged particle observables using modified Wood Saxon model in HIJING for U+U collisions at $\sqrt{s_{NN}} = 193$ GeV

S. K. Tripathy^{1,2}, M. Younus^{3, *}, Z. Naik², and P. K. Sahu¹

¹Institute of Physics, HBNI, Sachivalaya Marg, Bhubaneswar 751005, India

²Sambalpur University, Jyoti Vihar, Burla, Sambalpur 768019, India

³Indian Institute of Technology Indore, Simrol, Indore 453552, India

Abstract

We have implemented spherical harmonics in default Wood Saxon distribution of the HIJING model and calculated various physical observables such as transverse momentum, charged particle multiplicity, nuclear modification factor and particle ratios for charged particles at top RHIC energy with collisions of Uranium (U) nuclei. Results have been compared with available experimental data. We observe that, a particular type of collision configuration can produce significant magnitude change in observables. We have noticed that the tip-tip configuration shows higher magnitude of particle yield in central collisions, while the body-body configuration shows higher value in the cases of peripheral collisions, with the flip in the trend occurring for the mid-central U+U collisions.

Keywords : Monte Carlo simulations, deformed nuclei, Charged particle production

PACS: 21.60.Ka, 25.75.Dw

1 Introduction

Experiments with relativistic heavy ion collisions have shown formation of a hot and dense system of deconfined quarks and gluons commonly known as quark gluon plasma (QGP). Recent experiments with state-of-the-art technology involving gold (Au) and lead (Pb) nuclei are being conducted both at RHIC-BNL and LHC-CERN. While experimental data tends to reconstruct the entire heavy ion collision scenario from finally produced hadrons and leptons etc., theoretical and phenomenological models could calculate the final outcome by incorporating various analytical methods starting from the initial conditions of relativistic heavy ion collisions. It has been observed that initial conditions determine the evolution of quark gluon plasma and many of the final observables such as particle flow and correlations bear the signatures of such effects [1, 2]. Thus precise determination of initial conditions should play a vital role in explaining experimental observables. Theoretically it is assumed that heavy ions such as Au or Pb are almost spherical and have negligible or zero deformations. In order to have precise determination of the nature of initial conditions for different configurations, intrinsically deformed nuclei such as uranium (U) plays a vital role. The initial cold nuclear matter effects such as partons or nucleons multi-scattering when two nuclei collide may show certain orientation dependencies. Similarly, initially produced particles should also depend upon number of binary collisions of nucleons, and that too should depend on the orientations of the two colliding nuclei.

*younus.presi@gmail.com

In case of Au (mildly deformed) or Pb (zero deformation), we use Wood-Saxon (WS) distribution to define the distribution of nucleons within the nucleus. For the intrinsically deformed nucleus such as prolate shaped uranium, U, we have included n^{th} ordered deformation parameter, β_n , associated with spherical harmonics, $Y_{nl}(\vartheta)$, in the WS function [3–7]. The modified distribution is called modified Wood-Saxon (MWS) density distribution for the nucleons within the nucleus. MWS distribution is used as initial nucleon density in U+U collision in order to explain the experimental data. We have tried to use MWS in the context of Glauber formalism within the HIJING model to calculate charged particle multiplicities, transverse momentum distribution of charged particles etc., for tip on tip, body on body and random configuration collisions of uranium nuclei.

The paper is organised as follows. In Sec. 2 we have shown optimisation of MWS parameters to get the best values for the charged particles distribution, using HIJING code. This is followed by Sec. 3 on the results and their discussion. We finally summarise our results on Sec. 4.

2 Formalisms

Modified Wood Saxon distribution (MWS) distribution

In phenomenological approach for many body system, nuclear charge density is usually interpreted in a three parametric Fermi distribution [8].

$$\rho(r) = \rho_0 \left[\frac{1 + w(r/R)^2}{1 + \exp[(r - R)/a]} \right]. \quad (1)$$

Here ρ_0 is the nucleon density in the centre of the nucleus, R is the radius of the nucleus from its centre, and it is assumed that nucleon density reduces to the half of its maximum value at this distance. The parameter, a , is the skin depth or surface thickness, r is a position parameter and distance of any point from centre of the nucleus, and w is the deviation from a smooth spherical surface.

Au^{197} or Pb^{208} nucleus is assumed here to have uniform distribution of nucleons in its approximately spherical volume so that w can be taken to be zero. This reduces eqn.1 to the popular Wood-Saxon [9] distribution, which is used in most of the event generators for heavy-ion collisions. This may be written as:

$$\rho(r) = \frac{\rho_0}{1 + \exp[(r - R)/a]}. \quad (2)$$

When we use an axially symmetric or prolate deformed nucleus (viz. U^{238}), nuclear radius may be modified to include spherical harmonics as well. The deformed Wood-Saxon nuclear radius [10] may be written as:

$$R_{A\Theta} = R[1 + \beta_2 Y_{20}(\vartheta) + \beta_4 Y_{40}(\vartheta)] \quad (3)$$

Where the symbols β_i are deformation parameters,

ϑ is the polar angle with respect to the symmetry axis of the nucleus.

The spherical harmonics, Y_{20} , is given by [16],

$$Y_{20}(\vartheta) = \frac{1}{4} \sqrt{\frac{5}{\pi}} (3 \cos^2 \vartheta - 1) \text{ and } Y_{40}(\vartheta) = \frac{3}{16\sqrt{\pi}} (35 \cos^4 \vartheta - 30 \cos^2 \vartheta + 3).$$

Variables used in this Modified Wood Saxon distribution are listed in Table 1 along with their values taken from the references given in there. A study by Schenke et al [17] showed that, the variation in $0 < \beta_4 < 0.093$ has negligible effect on the nucleon distribution.

| Set | R (fm) | a | β_2 | β_4 |
|-----|---|---------------|------------|------------|
| 1 | $1.19 \times A^{1/3} - 1.16 \times A^{-1/3}$ [HIJING] | 0.54 [HIJING] | 0.215 [14] | 0.093 [14] |
| 2 | 6.86 [12] | 0.42 [12] | 0.265 [12] | NA |
| 3 | 6.81 [13] | 0.55 [13] | 0.28 [13] | 0.093 [13] |

Table 1: Different parameter sets for modified Wood-Saxon distribution

Event generator model, HIJING

Heavy Ion Jet Interaction Generator (HIJING) [11] program is designed explore possible initial conditions that may occur in relativistic heavy-ion collisions. HIJING assumes nucleus-nucleus collision which can be decomposed into binary nucleon-nucleon collisions. It uses a three-parameter Wood-Saxon nuclear density to compute the number of binary collisions at a given impact parameter. Between each pair of colliding nucleons, impact parameter is calculated using their transverse positions. Eikonal formalism, which uses straight line trajectories between two nucleons, is used to calculate probability of collision. Once all binary collisions are processed, then scattered partons in the associated nucleons are connected with the corresponding valence quarks to form string systems. Finally, particles are formed from the fragmentation of these strings. PYTHIA subroutine is used to generate kinematic variables for each semi/hard scattering.

We have implemented MWS formalism in HIJING model as mentioned in Eq. 3. Here we have taken random angle orientation of colliding nuclei along with two specific orientations, viz body-body ($\vartheta=0$) and tip-tip ($\vartheta=\pi/2$).

We have taken top RHIC energy (U+U $\sqrt{s_{NN}}=193$ GeV) and charged particles in our calculations.

In HIJING, participating and colliding nucleons numbers, N_{part} , and N_{coll} have been calculated using Glauber model in optical approximation. One can show from the Ref [18], these values as function of impact parameter or centralities,:

$$T_{AB}(b) = \int T_A(s) \cdot T_B(|s - b|) d^2s, \quad (4)$$

where, $T_{AB}(b)$ is the nucleus overlap function at a given impact parameter, b . Therefore, the no. of nucleon binary collisions in $A + B$ collisions, is given by

$$N_{coll}(b) = A \cdot B \cdot T_{AB}(b) \cdot \sigma_{NN}, \quad (5)$$

and the no. of participants is given by,

$$\begin{aligned} N_{part}(b) = & A \cdot \int T_A(s) \cdot \{1 - [1 - T_B(|s - b|) \sigma_{NN}]^B\} \cdot d^2s \\ & + B \cdot \int T_B(|s - b|) \cdot \{1 - [1 - T_A(s) \sigma_{NN}]^A\} \cdot d^2s, \end{aligned} \quad (6)$$

where σ_{NN} is the inelastic nucleon-nucleon cross section measured for a given collision energy of two nucleons. A and B are the mass numbers of the two colliding nuclei.

3 Results and discussions

In Fig. 1a, we have varied, a , β_2 and R parameters of Modified Wood Saxon function as mentioned in Table 1 to check their impact on nucleon distribution. For the first two sets of above parameters, 2nd order or 4th order deformation gives similar results of nucleon distribution.

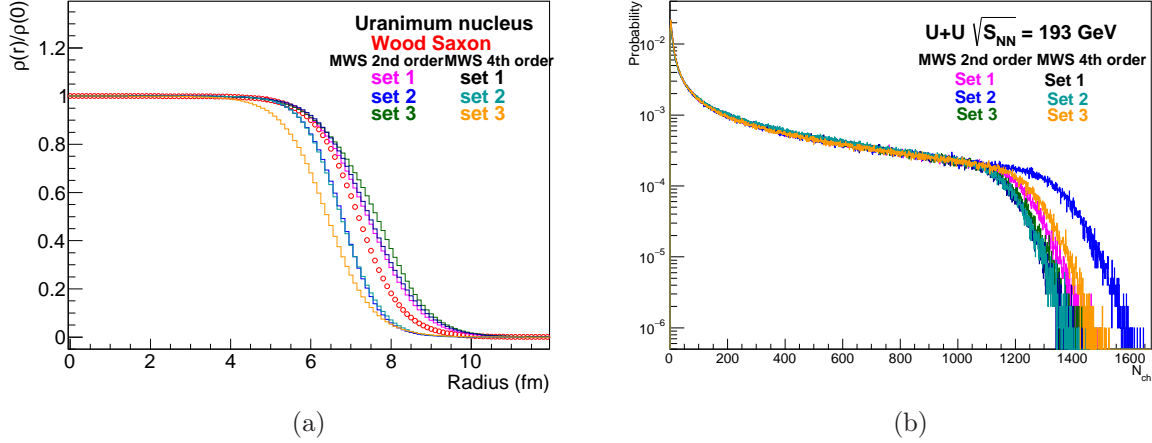


Figure 1: (Color online) Nucleon density distribution for Wood-Saxon and Modified Wood Saxon in Uranium nucleus are shown in Fig. 1a. Using the same sets parameters and orders of quadruple deformation, charged particle probability distribution shown in Fig 1b.

However, the 3rd set of parameters shows different distributions for different orders of quadruple deformation. To check how the values behave for charged particle production and which parameter set will yield results closer to experimental value, we have implemented these 3 sets of parameters in HIJING and results are shown in Fig. 1b. Although for the central part of the nucleus, different sets give the same value for the flat part of nucleon distributions, few set of parameter drop more rapidly than others. We observe that with 4th order deformation, set 1 and set 2 produce results closer to each other. Along this we also find that the 2nd order deformation with 3rd set of parameters do produce similar results to 4th order deformation, set 1. Hence, within the default HIJING parameters, we have preferred the set 1 and 4th order deformations (see Table – 1).

In Fig 2, we have shown charged particle multiplicity (N_{ch}) distribution from HIJING using Wood Saxon and Modified Wood Saxon density distribution. Only minimum-bias and mid-rapidity ($|\eta| < 0.5$) particles are considered here. Although N_{ch} shapes are consistent in all formalism, WS distribution lies between, body-body and tip-tip configurations of MWS. While body-body configuration yields least no. of charged particles, $n_{ch} \approx 1200$ among all configurations, tip-tip configuration gives $\sim 25\%$ higher charged particles than body-body configuration and gives the maximum value. We observe that Modified Wood Saxon distribution with random orientation of nuclei, gives similar results to that of non-deformed nuclei distribution. However, greater statistics is required to discern between the two. In the same figure, we have plotted the charged particle distribution for Au+Au collisions at $\sqrt{s_{NN}} = 200$ GeV and compared it with U+U collisions. Although, the trend of the distributions at the high multiplicity region in case of Au+Au collisions differs from that of U+U collisions for most of the orientations of Uranium nuclei, it is quite similar to the body-body collisions of the Uranium nuclei.

In Fig 3a, we have shown pseudo-rapidity distribution ($dN_{ch}/d\eta$) in most central collisions (0-5%) from HIJING using Wood Saxon and Modified Wood Saxon density distribution. We also identify the similar trend in this figure as observed among different orientations or configurations in Fig 2. In Fig 3b, we have $dN_{ch}/d\eta$ as a function of centrality. We observe that most central collision produces $dN_{ch}/d\eta \sim 1200$, while most peripheral collision produce ~ 200 . Tip-tip collision produces highest number of particles in most central collisions, while for the peripheral collisions, body-body configuration produces slightly more number of particles than the tip-tip. This trend however reverses around 10-20% centrality. Here, too we have shown pseudo-rapidity distribution of charged particles from Au+Au collisions. In the right-hand figure, the Au+Au results appear to be closer to the PHENIX data for the higher centrality collisions, which may

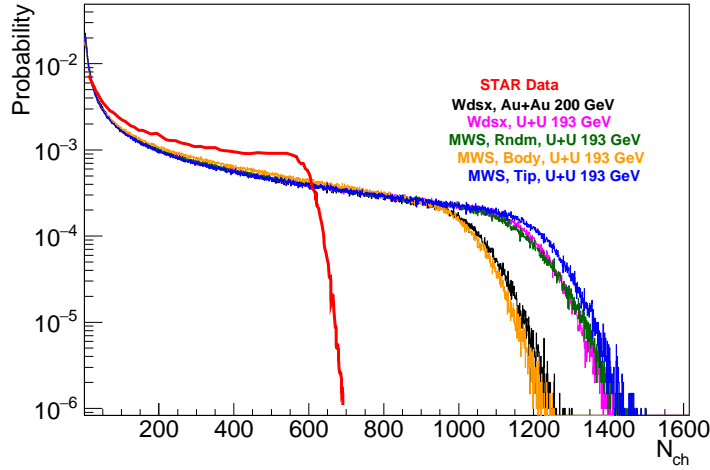


Figure 2: (Color online) Charged particle distribution using Wood Saxon and Modified Wood Saxon (MWS) for U+U collisions at $\sqrt{s_{NN}} = 193$ GeV and Au+Au collisions at $\sqrt{s_{NN}} = 200$ GeV in HIJING along with experimental data for U+U at $\sqrt{s_{NN}} = 193$ GeV. Two specific orientations viz. body-body ($\vartheta = \pi/2$) and tip-tip ($\vartheta = 0$) are shown along with random ϑ .

indicate that for collisions at the high centralities deformations in the nuclei may not play a large role. Here, for our model calculations we haven't assumed any deformation for the Gold (Au) nucleus.

In Fig 4, we have plotted $\langle p_T \rangle$ as a function of centrality. Here we observe very little dependence on centrality. In earlier paper by Rihan et al [4], where in the AMPT formalism, the dependence of average transverse momentum on orientation becomes more visible for more central collisions. We will keep investigating this difference on our future work. For most central collisions it is 0.42 GeV, while it was 0.4 GeV for most peripheral collisions. Similar to Fig 3b, $\langle p_T \rangle$ from tip-tip collision found to be higher in most central collision. Here the mean p_T of the charged particles observed from Au+Au collisions remains closer in the shape and magnitude to the tip-tip configurations of U+U collisions.

In Fig 5 we have plotted transverse momentum spectra at the most central (0-5%) and most peripheral collisions (60-80%) in Wood Saxon (magenta) and Modified Wood Saxon distribution in the top plot. In the bottom, ratio of these various types of configuration to the standard Wood-Saxon is presented. In Fig. 5a we observe that, MWS random configuration in U system yields similar magnitude results with WS (non-deformed) U nucleus and very little depends on centrality. While peripheral tip yields 30% higher magnitude, peripheral body goes 50% lesser magnitude. When we compare MWS U nucleus results with non-deformed Au nucleus result in Fig. 5b, we see peripheral body configuration can give 70% lesser magnitude while peripheral random configuration may give 40% lesser magnitude. Rest of configuration may give similar magnitude with Au nucleus results. Although there is magnitude fluctuation with non-deformed nucleus results (U or Au), we observe the ratio goes smooth with transverse momentum and centrality.

In Fig 6 we have presented nuclear modification factor as a function of transverse momentum in Wood Saxon (magenta) and modified Wood Saxon (rest of the curves). We have used the following definition of nuclear modification (R_{CP}) in the current calculations, where peripheral collisions is assumed to be devoid of any thermalized systems,

$$R_{CP} = \frac{d^2N/dp_T dy / \langle N_{coll}^{cent} \rangle}{d^2N/dp_T dy / \langle N_{coll}^{Perph} \rangle}. \quad (7)$$

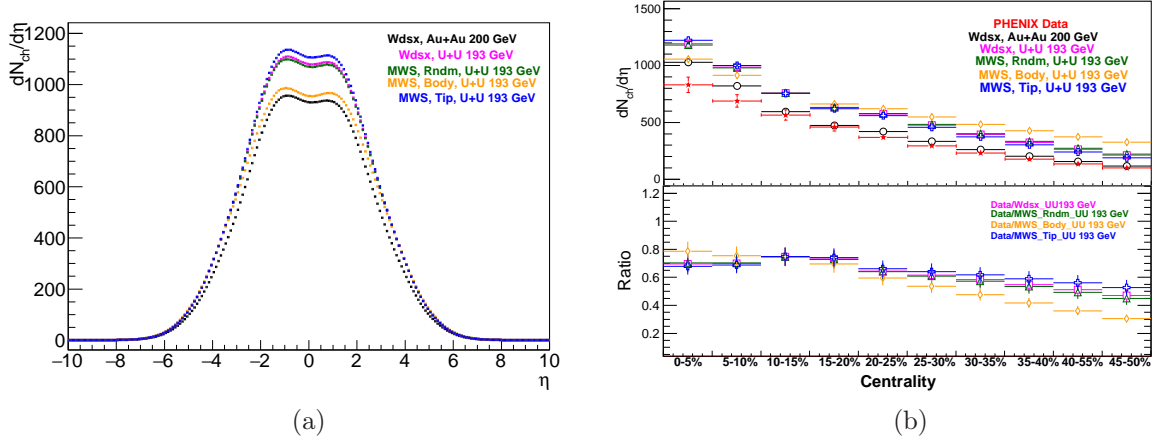


Figure 3: (Color online) In Fig 3a Pseudo-rapidity distribution using Wood Saxon and Modified Wood Saxon in HIJING is shown for U+U at $\sqrt{s_{NN}} = 193$ GeV and Au+Au at $\sqrt{s_{NN}} = 200$ GeV for 0-5% centrality. Two specific orientations viz. body-body ($\vartheta = \pi/2$) and tip-tip ($\vartheta = 0$) are shown along with random ϑ . Fig 3b shows $dN_{ch}/d\eta$ distribution using Wood Saxon and Modified Wood Saxon along with experimental data for U+U collisions at $\sqrt{s_{NN}} = 193$ GeV are shown as a function of centrality. Two specific orientations viz. body-body ($\vartheta = \pi/2$) and tip-tip ($\vartheta = 0$) are also shown along with random angle ϑ in the top plot. In the bottom plot, ratio of data to HIJING results are shown.

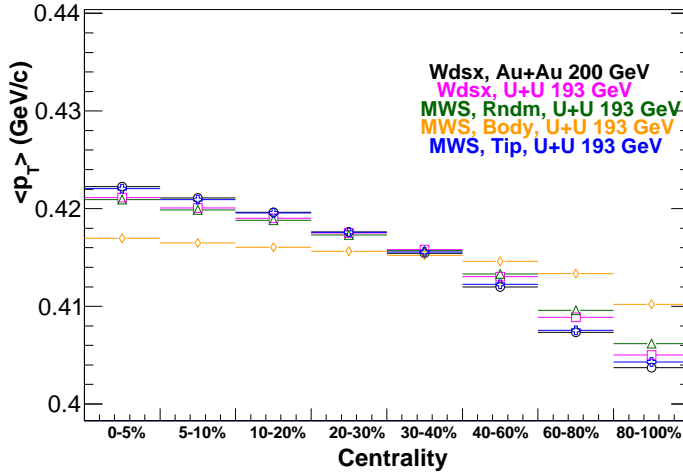


Figure 4: (Color online) $\langle p_T \rangle$ distribution using Wood Saxon and Modified Wood Saxon in HIJING for U+U collisions at $\sqrt{s_{NN}} = 193$ GeV and Au+Au collisions at $\sqrt{s_{NN}} = 200$ GeV. Two specific orientations viz. body-body ($\vartheta = \pi/2$) and tip-tip ($\vartheta = 0$) are shown along with random ϑ .

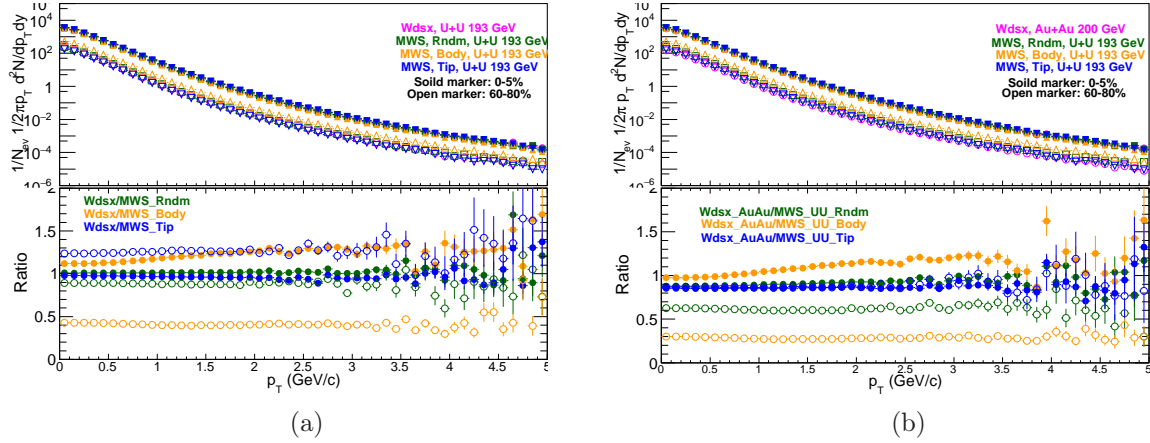


Figure 5: (Color online) (HIJING) Transverse momentum distribution using Wood Saxon and Modified Wood Saxon for U+U at $\sqrt{s_{NN}} = 193$ GeV and Au+Au collisions at $\sqrt{s_{NN}} = 200$ GeV. Two specific orientations viz. body-body ($\vartheta = \pi/2$) and tip-tip ($\vartheta = 0$) are shown along with random ϑ angle.

Where $\langle N_{coll}^{cent} \rangle$ and $\langle N_{coll}^{Perph} \rangle$ are average number of binary collisions in central (0-5%) and peripheral (60-80%) collisions, which have been calculated using Glauber model.

We observe that tip-tip configuration system is least modified, while system resulting from body-body collisions is affected most. We have used the nuclear shadowing parametrization incorporated in HIJING as well as energy loss mechanisms defined within the code. The energy loss depends on the rate of induced bremsstrahlung when any particle moves through the hot and dense partonic matter. The interaction points with the medium particles to calculate energy loss dE/dl , are determined by the probability,

$$dP = \frac{dl}{\lambda_s} e^{-dl/\lambda_s}, \quad (8)$$

where λ_s is the mean free path and dl is the elementary path-length traveled by the particle in QGP. The energy loss is then given by, $\Delta E = dl * dE/dl$.

The fact we observed from the Fig 6 is that the energy loss depends on the orientation of the colliding uranium nuclei. On the other hand the cold nuclear matter effects such as shadowing which manifests itself at low p_T (< 1 GeV), seems to be affected by the orientations of the colliding nuclei as well. In the figure, the tip-tip configuration shows least suppression while the body-body collision shows the most. This may be due to the fact that the QGP system size is smallest in case of tip-tip configuration while for the body-body configuration provides the biggest hot and dense matter, among all possible configurations. On the contrary, the shadowing effects is more prominent in the tip-tip configuration than in the body-body system. We guess that since the tip orientation (prolate uranium nucleus) in our calculations is assumed to be the major axis, it provides greater nuclear shadowing effects due to more number of available nucleons along this direction (i.e. major axis), whereas the body orientation is along the minor axis, it will cause the least shadowing effects on the particle spectra. Here, too the nuclear suppression for the random orientations of U nuclei is little more than standard WS configurations with zero deformity. On the other hand, Au+Au collisions assuming zero deformations show 20% less suppression when compared to U+U collisions with zero deformations which clearly present the system size dependencies on the particle energy loss and suppressions.

In Fig 7a we have plotted p/π and k/π ratio for most central collisions (0-5%) as a function of p_T . From $p_T > 1$ GeV onward, the trend of k/π ratio reverses and goes towards saturation faster than p/π ratio. In Fig 7b we have presented anti-particle to particle ratios π^-/π^+ , k^-/k^+ and \bar{p}/p as a function of p_T in most central collisions (0-5%). While pions give an almost flat

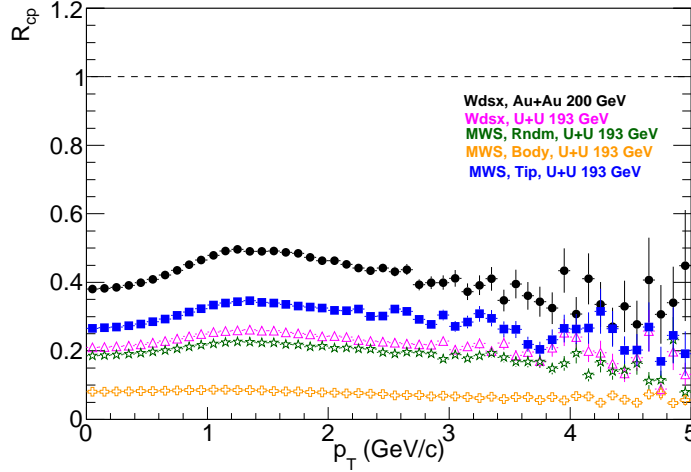


Figure 6: (Color online) (HIJING) Nuclear modification factor distribution using Wood Saxon and Modified Wood Saxon for U+U collisions at $\sqrt{s_{NN}} = 193$ GeV and Au+Au collisions at $\sqrt{s_{NN}} = 200$ GeV. Two specific orientations viz. body-body ($\vartheta = \pi/2$) and tip-tip ($\vartheta = 0$) are shown along with random ϑ .

ratio close to unity, others particle ratios decrease from unity for $p_T > 1$ GeV. We do not observe any orientation or collision configuration dependencies in either of the ratio plots, and the ratio values are found to be similar to non-deformed Wood Saxon measurements. Similarly, when the particle ratios from Au+Au collisions is compared to U+U collisions at almost same c.m. energies, we do not find any discernible effects of the system (QGP) on the particle ratios. We will continue to investigate the effects of system sizes on the particle production in our future works.

4 Summary

In this paper we have implemented Modified Wood Saxon distribution within HIJING formalism and calculated some physical observables for charged particle at RHIC energy, U+U at $\sqrt{s_{NN}} = 193$ GeV. We have used two particular orientations of colliding uranium nuclei, viz. tip-tip and body-body along with random azimuthal angle rotation. For comparison purposes, we have also shown results assuming zero deformation in uranium nucleus. Comparisons are also made with experimental data wherever available.

N_{ch} distribution in random configuration gives closer values to that Wood Saxon however larger statistics might be required to discern the fine disagreements between the two. We also notice that body-body configuration yields lesser particles while tip-tip shows higher production of charged particles. For central collisions, $dN_{ch}/d\eta$ in all configurations, gives similar deviation from data. While in peripheral collision, up to 30% variation is observed for body-body to tip-tip configurations. $\langle p_T \rangle$ shows trend among different configurations, which depends little of centrality. p_T spectra shows almost independent collision configuration in most central collision, while up to 50% deviation from Wood Saxon observed in tip-tip or body-body observed for peripheral collision. We have found R_{CP} depends upon the orientation and thus may imply that the extent of formation of hot and dense system depends upon the orientation itself. Particle ratios are found to be independent of collision configuration in most central collision. Furthermore, our studies with Au+Au as well as U+U collisions at the almost similar c.m. collision energies couldn't reveal any system size dependency on the observables such as particle ratios. However, energy loss suppression factor such as R_{CP} and transverse momentum spectra could reveal this dependency to some extent.

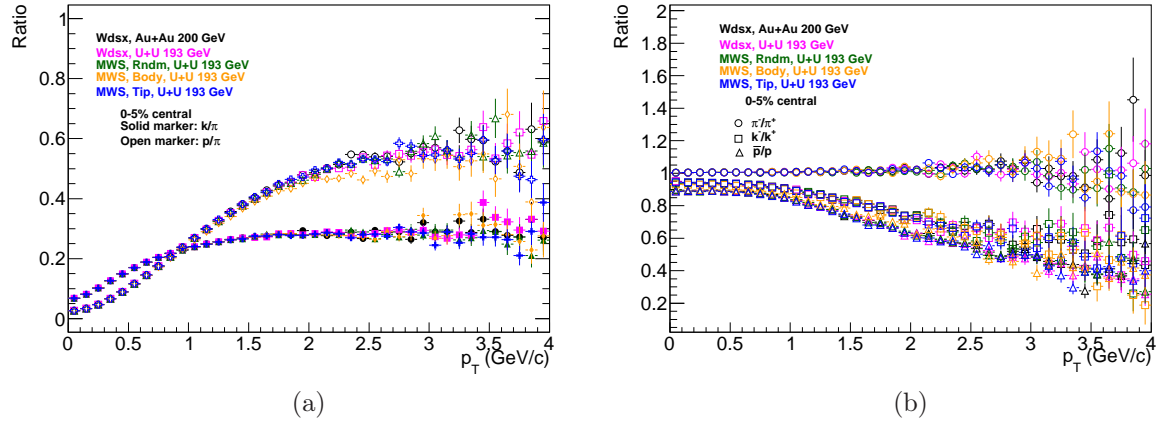


Figure 7: (Color online) (HIJING) Particle ratios using Wood Saxon and Modified Wood Saxon for U+U at $\sqrt{s_{NN}} = 193$ GeV and Au+Au at $\sqrt{s_{NN}} = 200$ GeV. Two specific orientations viz. body-body ($\vartheta = \pi/2$) and tip-tip ($\vartheta = 0$) are shown along with random ϑ

Our study shows that, tip-tip configuration can give us significant higher in magnitude than other configurations. While most central collisions are independent of collision configuration type, peripheral collisions may give an insight about this.

We aim to further extend this study in finding methods in selecting a particular type of configuration among all and give us indirect view of event-by-event analysis of U+U experimental data.

References

- [1] Raimond Snellings; New J.Phys. 13 (2011) 055008
- [2] Matthew Luzum and Hannah Petersen, J. Phys. G: Nucl. Part. Phys. 41 (2014) 063102
- [3] Hiroshi Masui, Bedangadas Mohanty and Nu Xu; Physics Letters B 679 (2009) 440-444
- [4] Md. Rihan Haque, Zi-Wei Lin and Bedangadas Mohanty, Phys. Rev C **85**, 034905 (2012)
- [5] Pingal Dasgupta, Rupa Chatterjee and Dinesh K. Srivastava Phys. Rev C **95**, 064907 (2017)
- [6] O.S.K. Chaturvedi et. al. Eur. Phys. J. Plus (2017) 132: 430
- [7] Arpit Singh et al, arXiv:1707.07552 [nucl-th]
- [8] R. Hofstadter, Nobel Lecture, December 11, 1961
- [9] Roger D. Woods and David S. Saxon, Phys. Rev. 95, 577, 1954
- [10] D.L. Hendrie, N.K. Glendenning, B.G. Harvey, O.N. Jarvis, H.H. Duhm, J. Saudinos, J. Mahoney, Physics Letters B Volume 26, Issue 3, Pages 127-130 (1968)
- [11] Miklos Gyulassy and Xin-Nian Wang, Comput.Phys.Commun. 83 (1994) 307; <http://ntc0.lbl.gov/~xnwang/hijing/>
- [12] Q.Y.Shou et al, Physics Letters B, 749,2015, Pages 215-220
- [13] Hiroshi Masui et al, Physics Letters B 679 (2009) 440-444

- [14] P.Moller, J.R.Nix, W.D.Myers and W.J.Swiatecki, Atomic Data and Nuclear Data Tables 59 185 (1995)
- [15] Schenke et al., PHYSICAL REVIEW C 89, 064908 (2014)
- [16] C 5, Quantum Theory of Angular Momentum, By D A Varshalovich, A N Moskalev, V K Khersonskii
- [17] Schenke et al., PHYSICAL REVIEW C 89, 064908 (2014)
- [18] Michael L. Miller, Klaus Reygers, Stephen J. Sanders, and Peter Steinberg, Annu. Rev. Nucl. Part. Sci. 2007. 57:205-243